SAND2011-4881C

High-Fidelity Atomistic Simulations of Melt-Growth of CZT Crystals

The 18th American Conference on Crystal Growth and Epitaxy

Monterey, CA, July 31-August 5, 2011

Xiaowang Zhou

Sandia National Laboratories

Project Team

X. W. Zhou, D. K. Ward, B. M. Wong, and F. P. Doty

Current Status in the Growth Simulation

1. Stillinger-Weber (SW) potentials are most widely used (~2300 citations);
2. Tersoff/Brenner potentials are second-widely used (~1300 citations);
3. Simulations of crystalline growth are limited to vapor deposition; convincing cases for melt-growth are yet to be demonstrated;
4. Most successful simulations of crystalline growth of vapor deposition were achieved using SW potentials;
5. Many Tersoff literature potentials were found to predict amorphous growth in vapor deposition simulations.

BOP Origin

* bond order: half the difference of electrons in the bond and anti-boding states.
\# bond integral: hopping probability of electrons from one orbital to another.

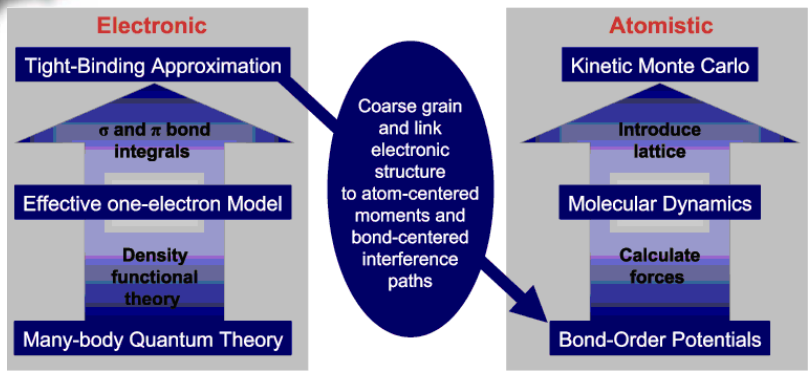

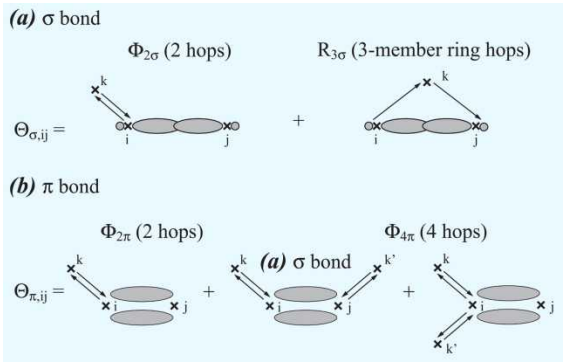

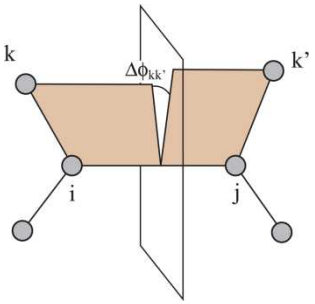

1. **Derived from quantum mechanics theory through systematic coarse-graining;**
2. **Separate treatment of σ and π bonding energies** (products of bond order* and bond integral#);
3. **The first two levels of the expanded Green function retained for the σ and π bond orders;**
4. **Up to four electron hops are considered, naturally incorporating the 3-member ring term in the σ bonding ($R_{3\sigma}$) and the dihedral angle ($\Delta\phi_{kk'}$) effect in the p bonding;**
5. **Valence effect is addressed.**
6. **Accuracy comparable to quantum mechanics and scale comparable to conventional molecular dynamics.**

1. D. G. Pettifor, M. W. Finnis, D. Nguyen-Manh, D. A. Murdick, X. W. Zhou, and H. N. G. Wadley, Mater. Sci. Eng. A, 365, 2 (2004).
2. D. G. Pettifor, and I. I. Oleinik, Phys. Rev. B, 59, 8487 (1999).
3. D. G. Pettifor, and I. I. Oleinik, Phys. Rev. Lett., 84, 4124 (2000).
4. D. G. Pettifor, and I. I. Oleinik, Phys. Rev. B, 65, 172103 (2002).
5. R. Drautz, D. A. Murdick, D. Nguyen-Manh, X. W. Zhou, H. N. G. Wadley, and D. G. Pettifor, Phys. Rev. B, 72, 144105 (2005).
6. D. A. Murdick, X. W. Zhou, H. N. G. Wadley, D. Nguyen-Manh, R. Drautz, and D. G. Pettifor, Phys. Rev. B, 73, 45206 (2006).

Sandia National Laboratories

BOP Goals

Accuracy comparable to quantum mechanics and scale comparable to conventional molecular dynamics

- **Bond order potential (BOP) is derived from quantum mechanics theories;**
- **We will develop a CdTe BOP and validate it against clusters** (dimer, trimer, square, tetrahedron, and chain for elements and compounds; Cd_2Te and $CdTe_2$ trimers for compounds)**, lattices** (diamond-cubic, simple-cubic, body-centered-cubic, face-centered-cubic, hexagonal-close-packed, graphite, graphene, and A8 for elements; zinc-blende, wurtzite, NaCl, CsCl, binary-graphite, AuCu, CuPt, NiAs, CrB, AlSb, binary-graphene, and face-centered-square for the stoichiometric compound CdTe; Ag_2O, CaF_2 for the non-stoichiometric compounds $CdTe_2$ or Cd_2Te)**, and defects** (vacancies, Cd@Te and Te@Cd antisites, Cd and Te interstitials at different locations)**;**
- **We will also validate the BOP using melt- and vapor- phase growth simulations** (ensure the lowest energy for the equilibrium phases by testing a variety of configurations that are not possible to study directly)**;**

BOP Captures Many Cd, Te, and CdTe Phases

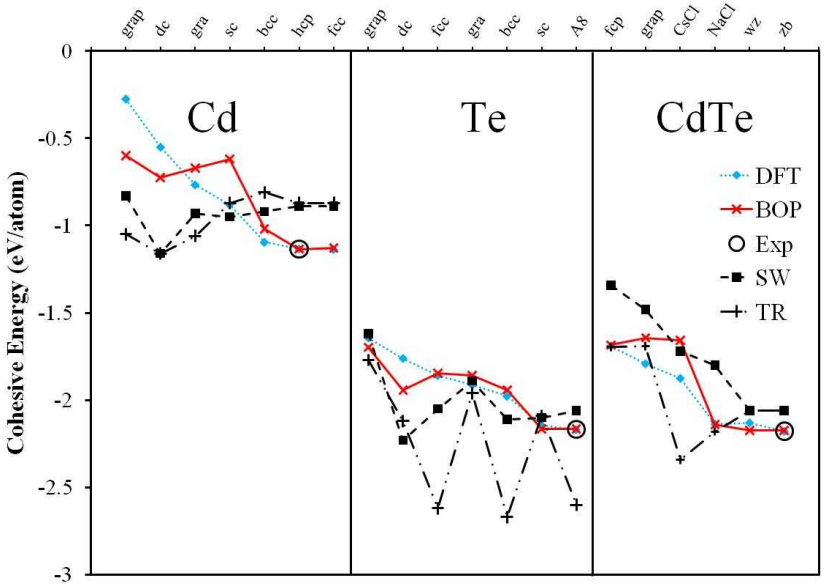

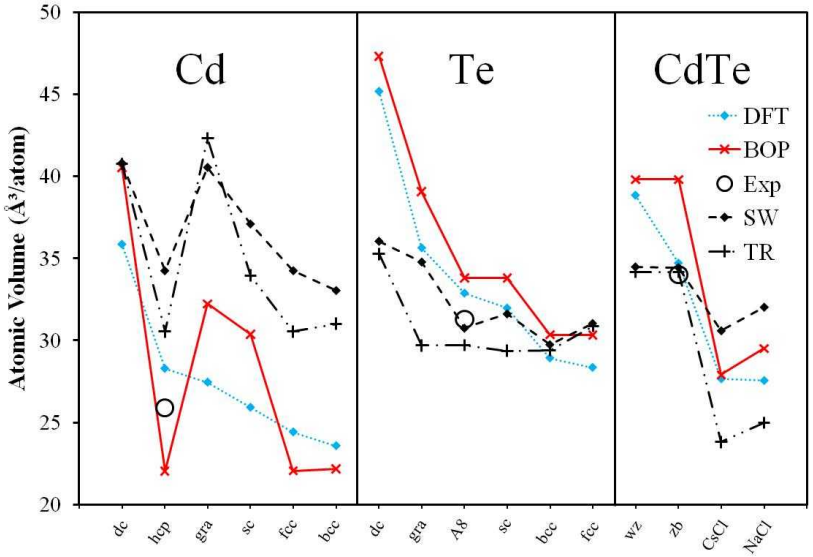

Have validated against clusters (dimer, trimer, square, tetrahedron, and chain for elements and compounds; Cd_2Te and $CdTe_2$ trimers for compounds)**, lattices** (diamond-cubic, simple-cubic, body-centered-cubic, face-centered-cubic, hexagonal-close-packed, graphite, planer-graphite, and A8 for elements; zinc-blende, wurtzite, NaCl, CsCl, binary-graphite, AuCu, CuPt, NiAs, CrB, AlSb, planar-binary-graphite, and face-centered-square for the stoichiometric compound CdTe; Ag_2O, CaF_2 for the non-stoichiometric compounds $CdTe_2$ or Cd_2Te)**, and defects** (vacancies, Cd@Te and Te@Cd antisites, Cd and Te interstitials at different locations)

An Example Vapor Deposition Simulation

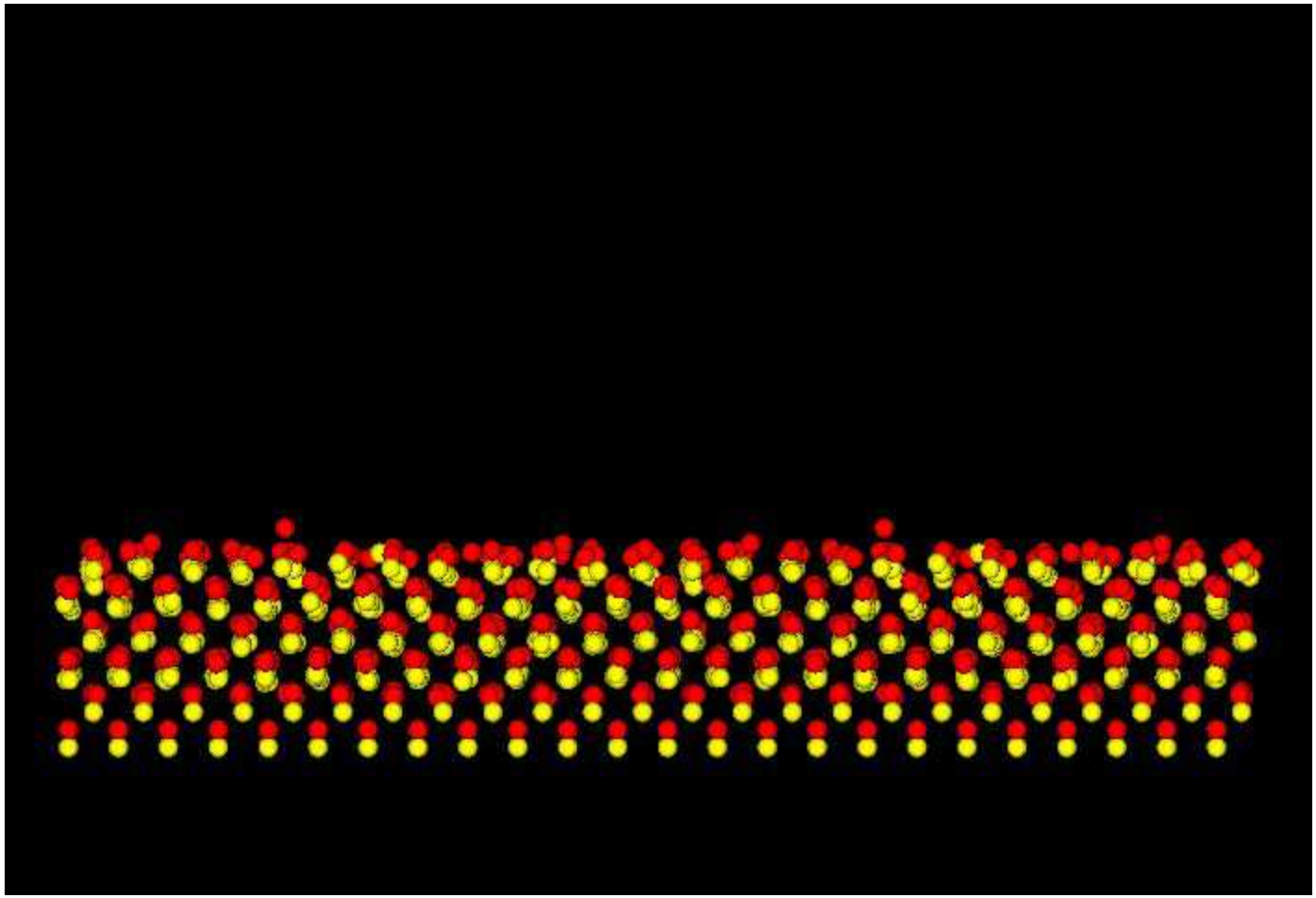

Substrate temperature 1200K; adatom energy 0.1 eV; vapor species Cd + Te_2; deposition rate 2.7 nm/ns

MD Simulations of Misfit Dislocation Formation

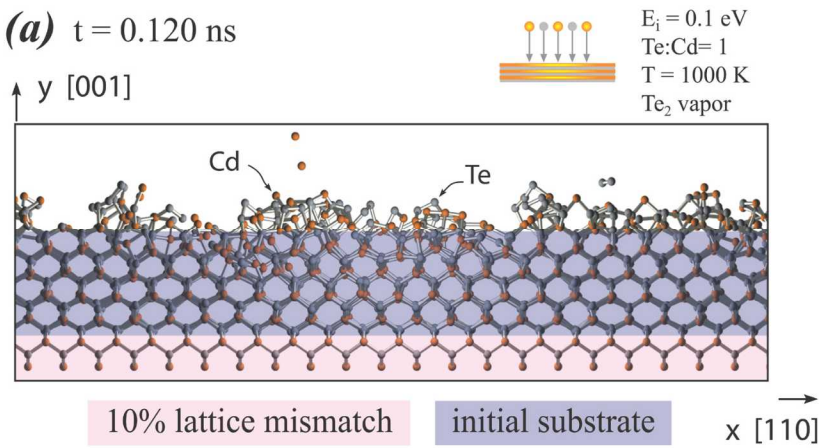

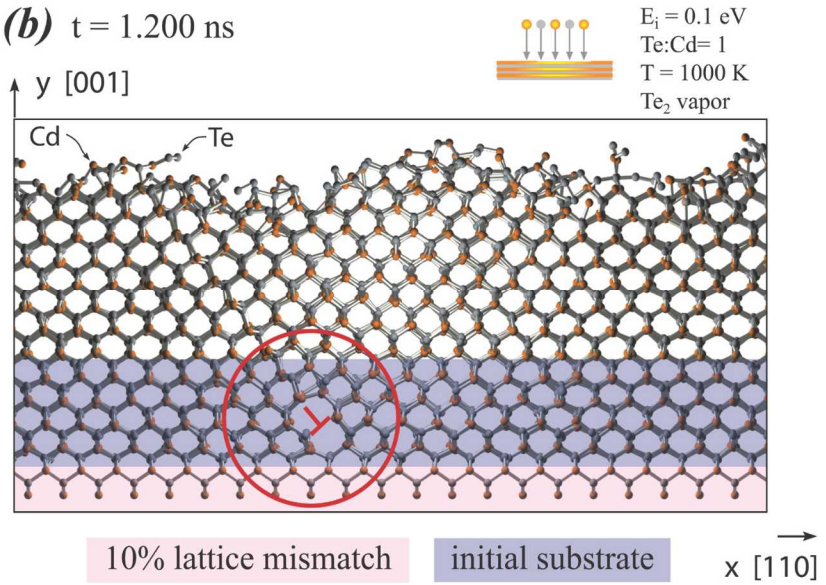

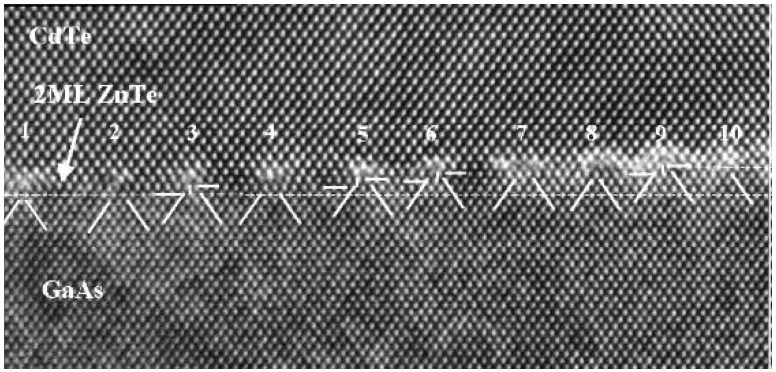

Similar misfit dislocation structures observed from HRTEM experiment in GaAs/ZnTe/CdTe samples. S. Kret, P. Dluzewski, P. Dluzewski, and J.-Y. Laval, Phil. Mag., 83, 231 (2003).

Sandia National Laboratories

MD Simulation of Melt-Growth of CdTe

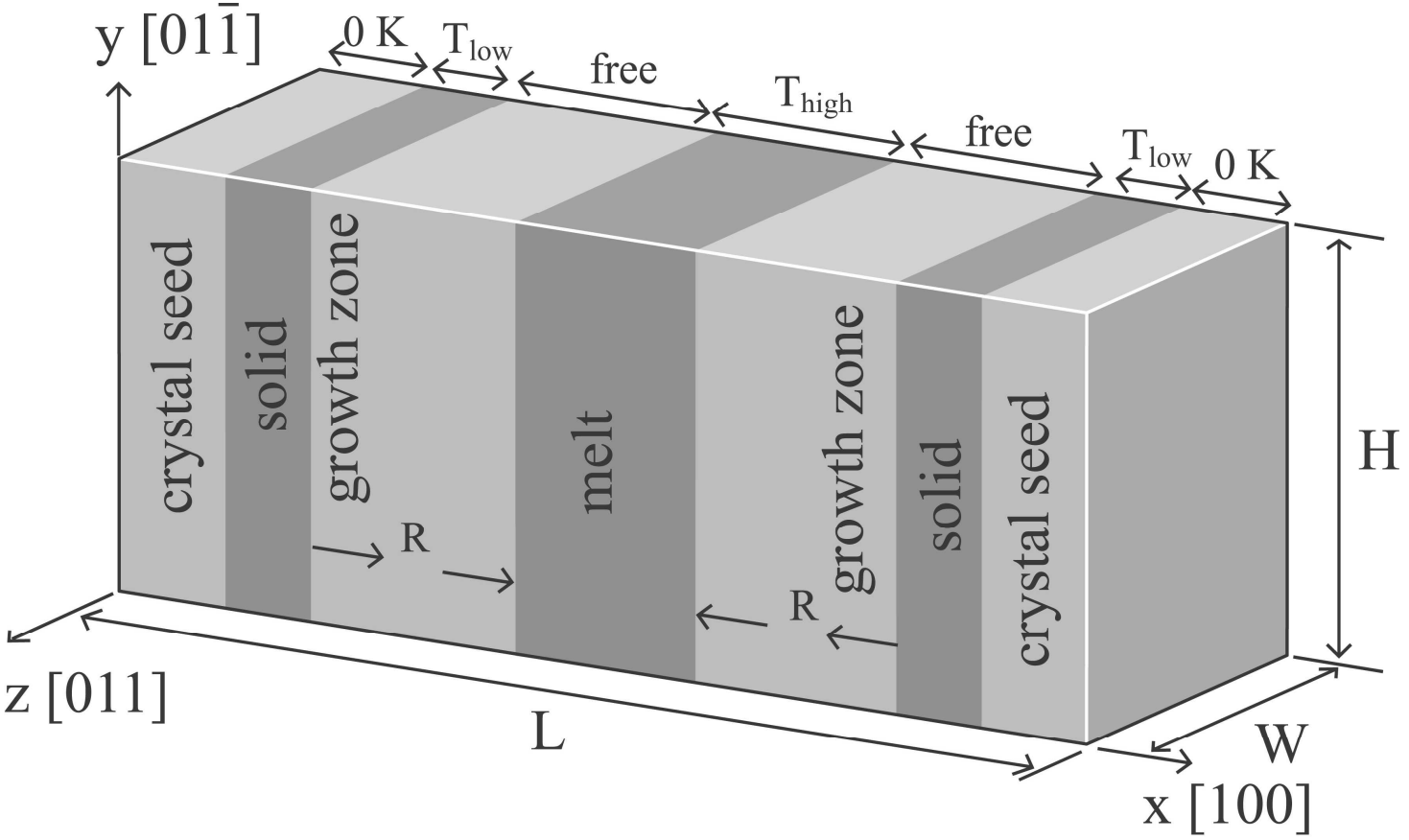

8

An Example at T_{low}=1000K, T_{high}=2200K, R = 0.2 Å/ps

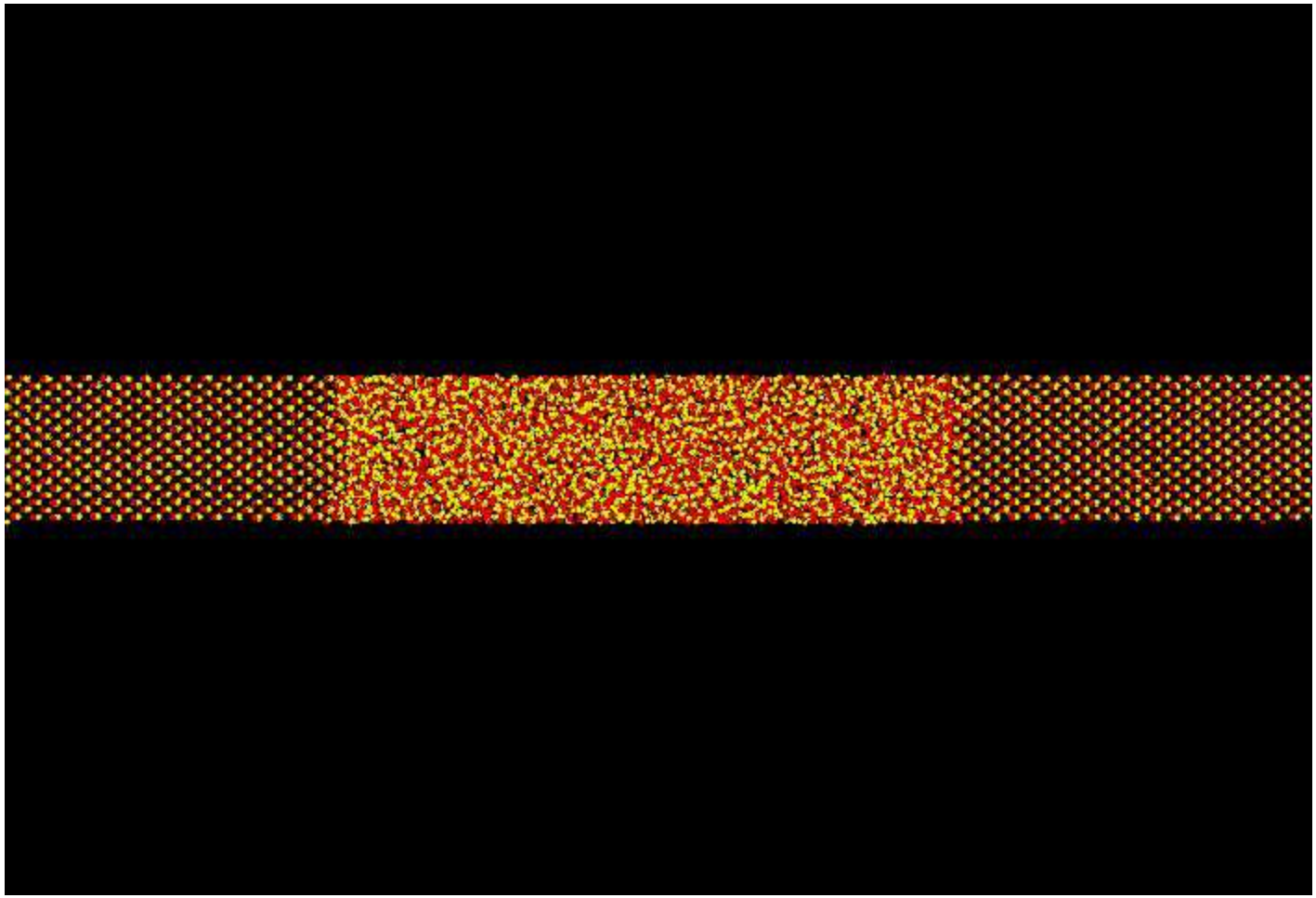

Growth Observation

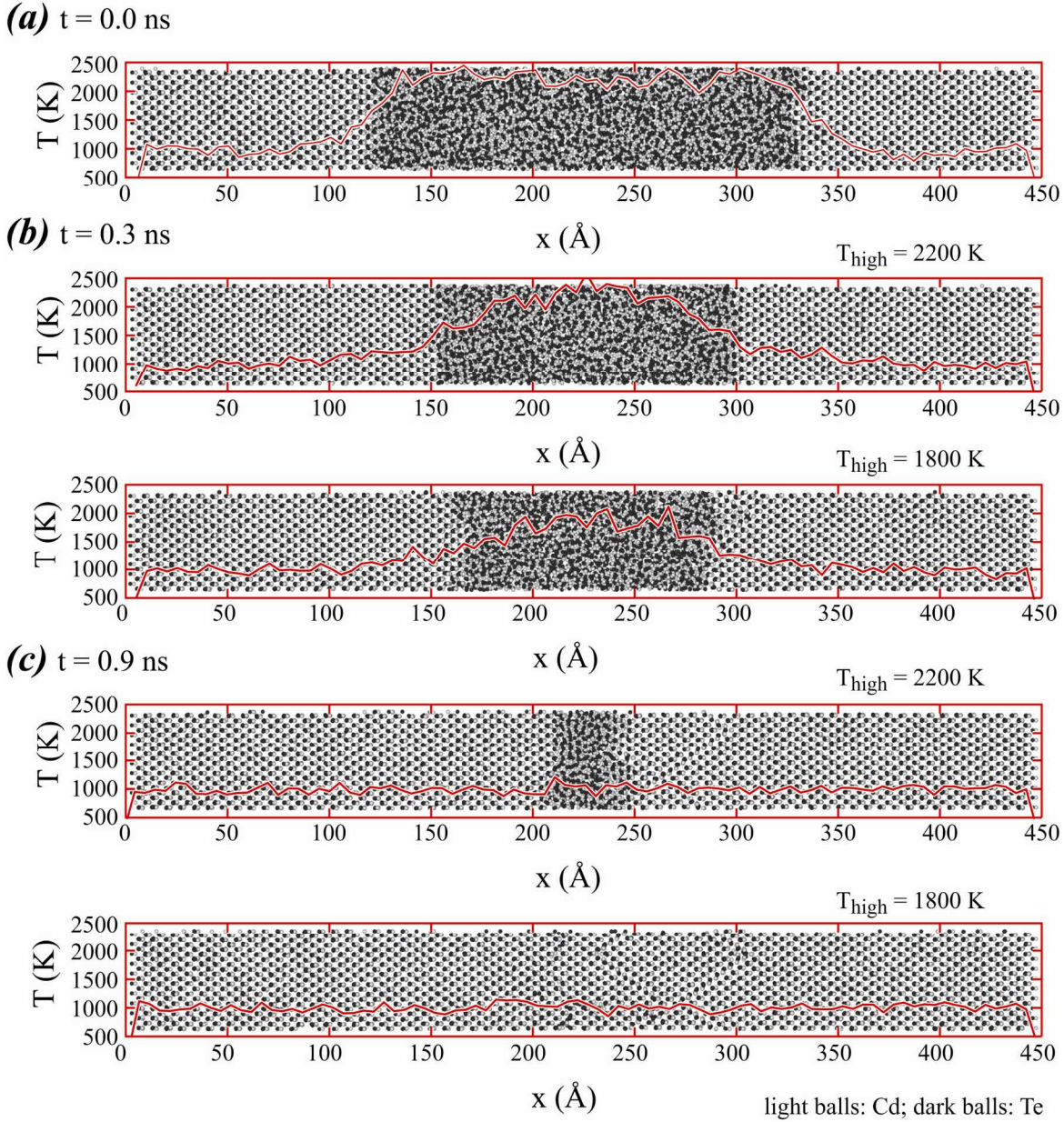

Sandia National Laboratories

Quality of the Grown Crystals

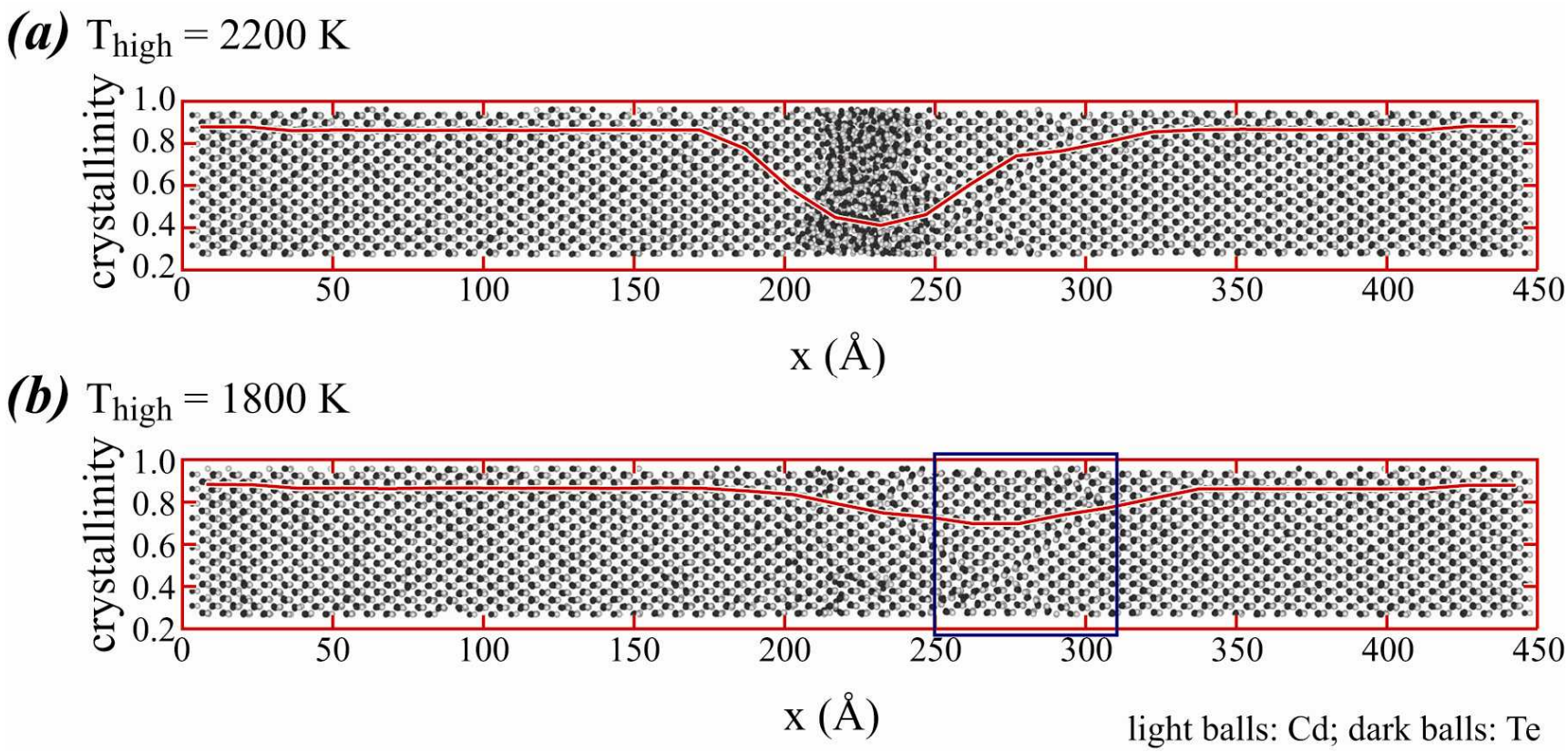

Discovery of Stacking Fault Defects

(a) framed region in Fig. 4(b)

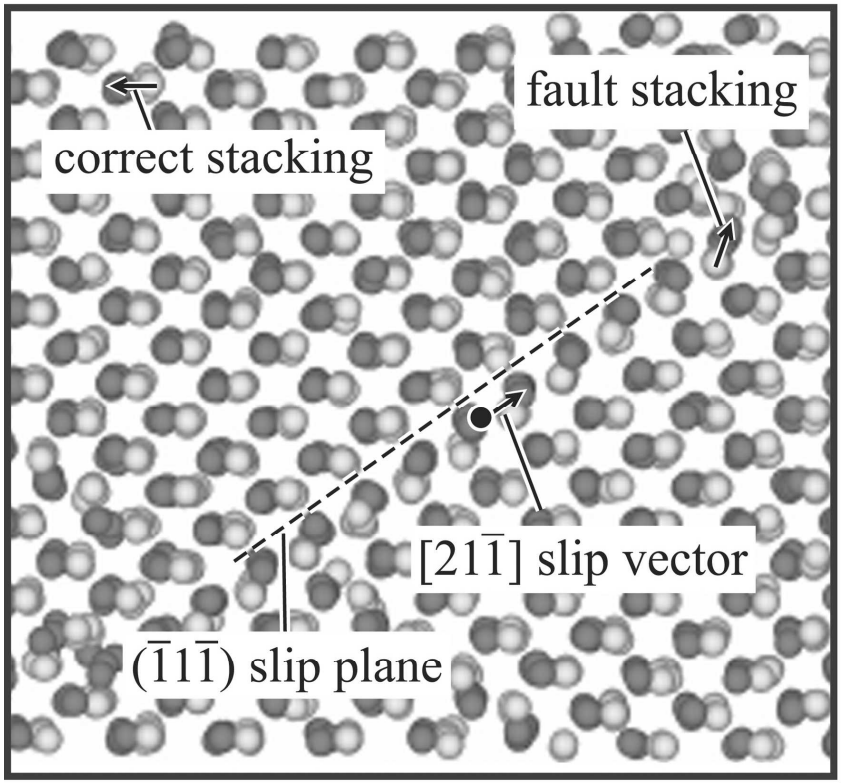

(b) defect nucleation at local facets

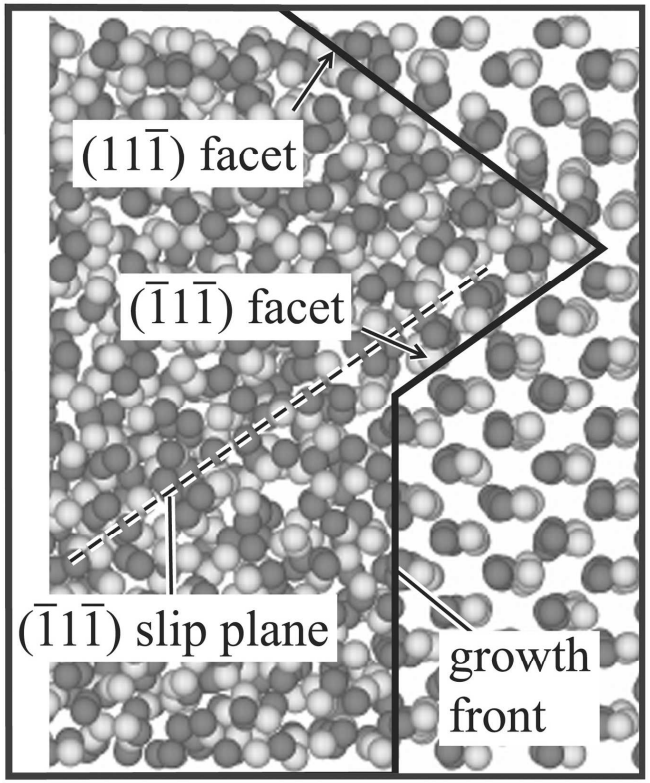

Conclusions

- **BOP enables an empirical MD scale and a quantum-mechanical fidelity;**
- **New BOP-based MD method simulates accurately CdTe melt-growth;**
- **Amorphous regions can be trapped and stacking faults can be nucleated on {111} planes during melt-growth.**

Acknowledgement

This work is supported by the NNSA/DOE Office of Nonproliferation Research and Development, Proliferation Detection Program, Advanced Materials Portfolio. Sandia National Laboratories is a multi-program laboratory managed and operated by Sandia Corporation, a wholly owned subsidiary of Lockheed Martin Corporation, for the U.S. Department of Energy's National Nuclear Security Administration under contract DE-AC04-94AL85000.

Ideal Atomistic Model for Growth

1. **Transferrable to a variety of configurations: clusters** (dimer, trimer, square, tetrahedron, and chain for elements and compounds; Cd_2Te and $CdTe_2$ trimers for compounds)**, lattices** (diamond-cubic, simple-cubic, body-centered-cubic, face-centered-cubic, hexagonal-close-packed, graphite, graphene, and A8 for elements; zinc-blende, wurtzite, NaCl, CsCl, binary-graphite, AuCu, CuPt, NiAs, CrB, AlSb, binary-graphene, and face-centered-square for the stoichiometric compound CdTe; Ag_2O, CaF_2 for the non-stoichiometric compounds $CdTe_2$ or Cd_2Te)**, and defects** (vacancies, Cd@Te and Te@Cd antisites, Cd and Te interstitials at different locations)**;**
2. **Lowest energy for the equilibrium structure;**
3. **Validatable in vapor- and melt- growth simulations: testing a variety of configurations that are not possible to study directly.**

Stillinger-Weber (SW) Potential

$$E = \frac{1}{2}\sum_{i}\sum_{j\neq i}\left[R_{ij}\left(r_{ij}\right)-U_{ij}\left(r_{ij}\right)\right]+\frac{1}{2}\sum_{i}\sum_{j\neq i}\sum_{k\neq j\neq i}u_{ij}\left(r_{ij}\right)\cdot u_{ik}\left(r_{ik}\right)\cdot\left[\cos\left(\theta_{jik}\right)+\frac{1}{3}\right]^{2}$$

$$\phi_{ij}\left(r_{ij}\right)=R_{ij}\left(r_{ij}\right)-U_{ij}\left(r_{ij}\right)=\begin{cases}\varepsilon_{ij}A_{ij}\left(\dfrac{B_{ij}}{r_{ij}^{4}}-1\right)\exp\left(\dfrac{\sigma_{ij}}{r_{ij}-a_{ij}\sigma_{ij}}\right) & , \quad r_{ij}\leq a_{ij}\sigma_{ij}\\ 0 & , \quad r_{ij}>a_{ij}\sigma_{ij}\end{cases}$$

$$u_{ij}\left(r_{ij}\right)=\begin{cases}\sqrt{\varepsilon_{ij}\lambda_{ij}}\exp\left(\dfrac{\gamma_{ij}\sigma_{ij}}{r_{ij}-a_{ij}\sigma_{ij}}\right) & , \quad r_{ij}\leq a_{ij}\sigma_{ij}\\ 0 & , \quad r_{ij}>a_{ij}\sigma_{ij}\end{cases}$$

ε_{ij}, λ_{ij},, γ_{ij}, A_{ij}, B_{ij}, σ_{ij}, a_{ij}, are parameters, and $\sigma_{ij}\cdot a_{ij}$ is cutoff distance.

F. H. Stillinger, and T. A. Weber, Phys. Rev. B, 31, 5262 (1985).

SW Potentials "Easily" Simulate Crystalline Growth

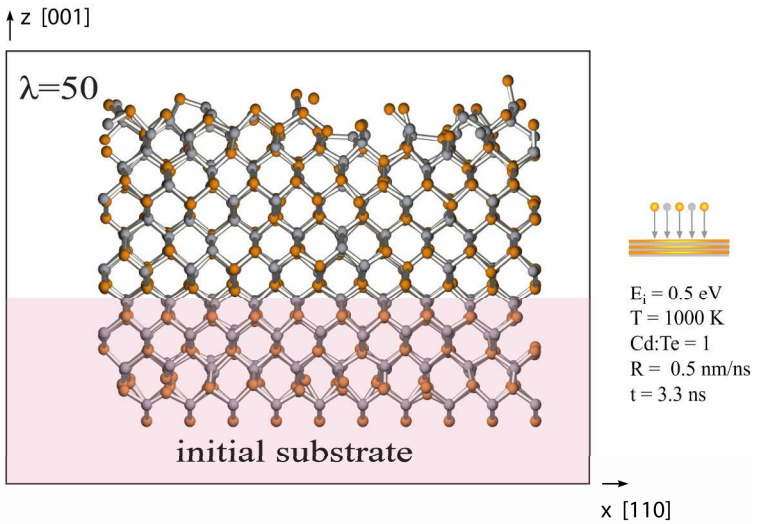

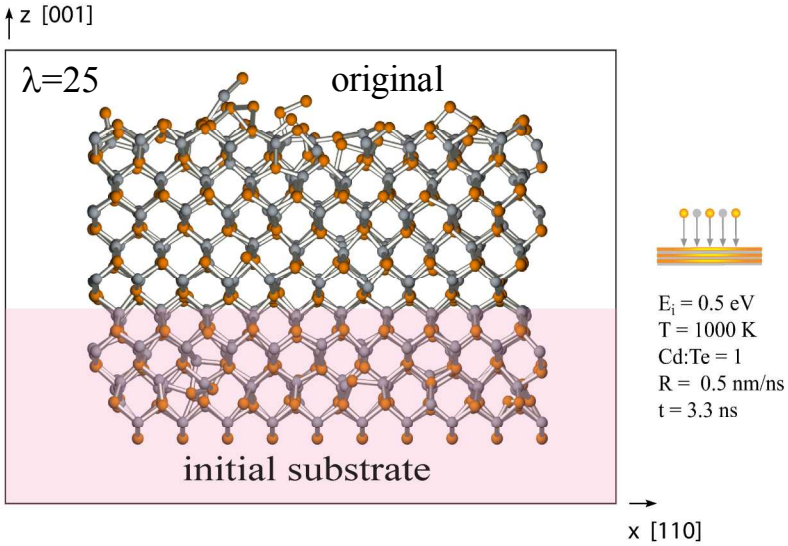

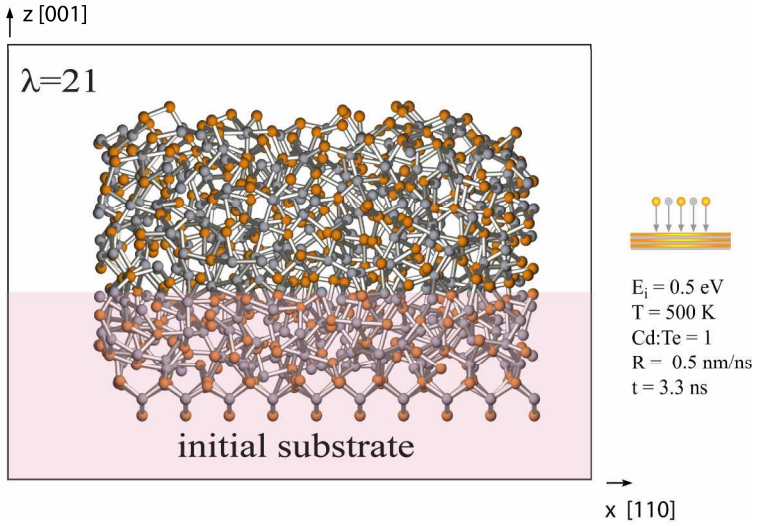

CdTe potential from Z. Q. Wang, D. Stroud, and A. J. Markworth, Phys. Rev. B, 40, 3129 (1989).

Other Properties

Elastic Constants of zinc-blende CdTe (GPa)

C_{ij}	experiment (300K)[1]	DFT[2]	BOP	Tersoff-Rockett[3]	Stillinger-Weber[4]
C_{11}	53.3	53.2	49.5	50.7	44.3
C_{12}	36.5	36.0	31.3	37.5	19.6
C_{44} (relaxed)	20.4	---	---	15.2	18.0
C_{44} (unrelaxed)	---	31.8	40.6	46.8	30.7

Defect energies of zinc-blende CdTe (eV)

defect type	DFT	BOP	Tersoff-Rockett[3]	Stillinger-Weber[4]
Cd vacancy	2.20	2.66	2.43	2.60
Te vacancy	2.72	1.64	0.93	1.53
Cd antisite	3.01	3.24	0.18	0.80
Te antisite	3.16	2.04	1.19	0.74
Cd in Cd interstitial	1.98	1.21	1.36	4.27
Te in Cd interstitial	3.52	2.92	0.55	2.60
Cd in Te interstitial	2.14	2.12	0.61	3.76
Te in Te interstitial	3.91	2.92	1.28	3.57

1. J. M. Rhowe, R. M. Nicklow, D. L. Price, and K. Zanio, Phys. Rev. B, 10, 671 (1974).
2. B. K. Agrawal, and S. Agrawal, Phys Rev. B, 45, 8321(1992).
3. J. Oh, and C. H. Grein, J. Crys. Growth, 193, 241 (1998).
4. Z. Q. Wang, D. Stroud, and A. J. Markworth, Phys. Rev. B, 40, 3129 (1989).

Cd and Te Vapor Growth Simulations

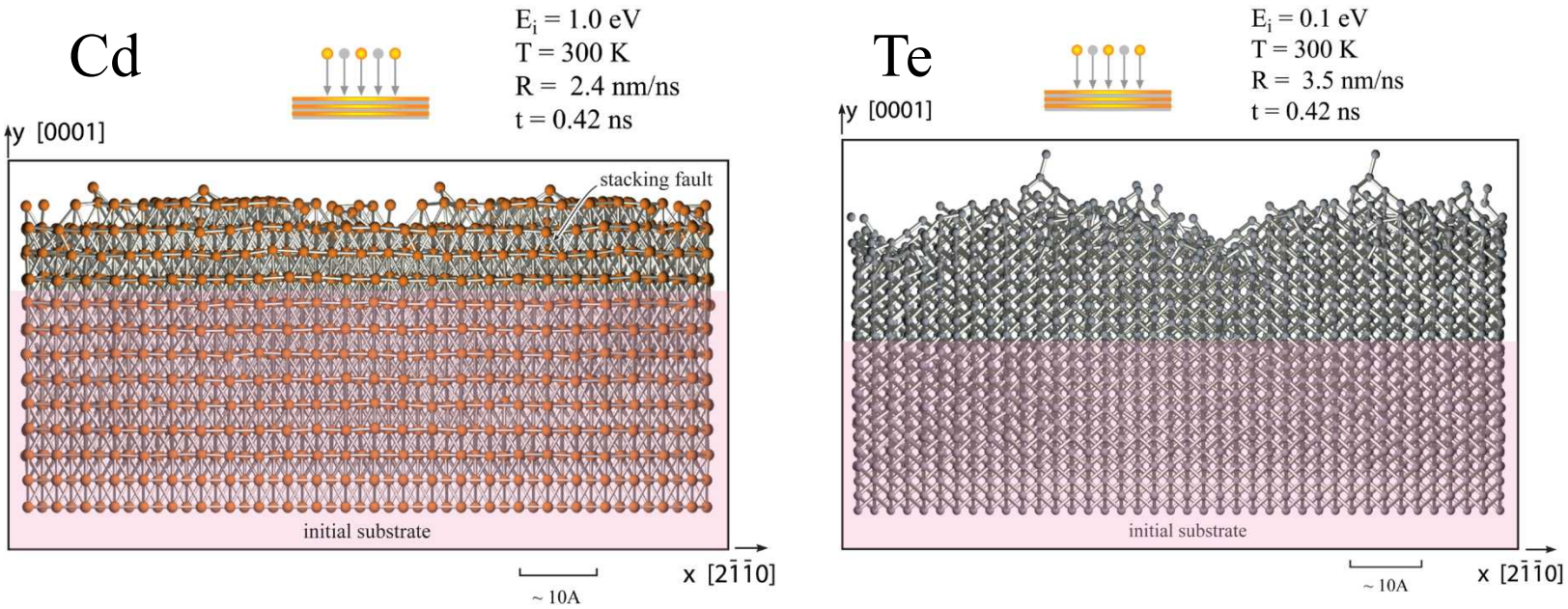

Crystalline growth was obtained for Cd and Te elemental growth as well as CdTe compound growth.